# From nanotubes to single crystals: Co doped TiO$_2$

J. Jaćimović, E. Horváth, B. Náfrádi, R. Gaál, N. Nikseresht,
H. Berger, L. Forró, and A. Magrez[a]
*Institute of Condensed Matter Physics (ICMP), Ecole Polytechnique Fédérale*
*de Lausanne, CH-1015 Lausanne, Switzerland*

Millimeter-sized cobalt doped rutile crystals with a bi-pyramidal shape are obtained by chemical vapour transport using scroll-type H$_2$Ti$_3$O$_7$ nanotubes as a precursor in which Co$^{2+}$ ions are introduced by a simple ion exchange method prior to the growth. Despite the low concentration of Co$^{2+}$ dopants ($5 \times 10^{19}$ cm$^{-3}$), the resistivity of the single crystal shows a metallic behaviour above 50 K and the Seebeck coefficient has the signatures of polaronic quasiparticles. The magnetic properties of the material show a weak anti-ferromagnetic interaction between the spins on Co atoms below 50 K. This synthesis method could be beneficial for the growth of a large variety of doped TiO$_2$ single crystals. *© 2013 Author(s). All article content, except where otherwise noted, is licensed under a Creative Commons Attribution 3.0 Unported License.* [http://dx.doi.org/10.1063/1.4820438]

Titanium dioxide, TiO$_2$, a wide band gap semiconductor, has a broad range of applications. A few, among others, are mesoscopic solar cells, photo-catalysis, diluted magnetic semiconductors (DMS), and thermoelectric devices.[1–3]

In all these applications, doping the host material is a central issue. In photo-catalysis, the goal is to reduce the band-gap and profit more from the visible solar spectrum.[4] In the case of the thermoelectric devices, the optimization of the material's properties for a high figure of merit is undertaken by doping studies.[5] Additionally, it has been reported that Co doped TiO$_2$ rutile has ferromagnetic (FM) characteristics, which places this compound into the family of DMS,[6] a potential candidate for spintronics applications. It has been claimed that the cobalt spins create a FM ground state above room temperature.[7–9] However, the microscopic mechanism of this interaction remains unresolved.

The major scientific effort thus far has been invested in the synthesis of Co doped thin films of TiO$_2$ to study the origin of the ferromagnetic interaction.[10] The quality of the films appears to be very important. The non-uniformity in the films leads to the absence of a ferromagnetic correlation, indicating that the growth and post-growth processing play an important role in the distribution of the Co atoms in the material.[11] The films which are considered to be homogenously doped exhibit ferromagnetism at room temperature, but its intrinsic origin is still under debate. Since it is difficult to unravel the leading physical properties in the case of grain boundaries, defects, and stoichiometry issues, one way to proceed in the understanding of DMS would be to grow Co doped TiO$_2$ single crystals.

Several attempts to grow Co-doped TiO$_2$ single crystals using anatase and transition metal oxide powders as a starting material in chemical vapour transport (CVT) method were made.[12] However, the homogeneity and the dopant concentration of the samples were not satisfactory. To overcome this obstacle, the strategy we apply is to use TiO$_2$ nanotubes[13] as a precursor material which are already homogenously doped with cobalt. In a previous work, we reported homogenous manganese doped titanate nanotubes.[14, 15] Here, we apply the same procedure to obtain a homogeneously Co-doped starting material for growing single crystals.

---

[a]Author to whom correspondence should be addressed. Electronic mail: arnaud.magrez@epfl.ch
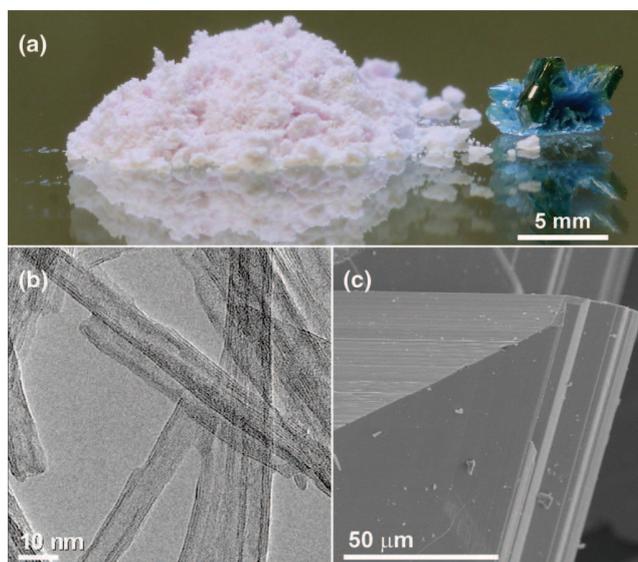
**1**, 032111-1

FIG. 1. (a) Photography of Co doped titanate nanotube powder starting material and a rutile $TiO_2$ single crystal. (b) TEM image of Co doped titanate nanotubes. (c) SEM micrograph of a Co doped rutile $TiO_2$ single crystal.

In this paper, we report on the chemical vapour transport assisted single crystal growth of cobalt doped rutile $TiO_2$ by using Co-doped titania nanotubes as a precursor. The detailed chemical analysis of the compound produced by this new method demonstrates the high quality of the starting material and of the single crystals as well. In addition to the composition and structure, we measured the temperature dependence of the resistivity and thermo-electric power and studied the magnetic properties by ESR and SQUID measurements. To our knowledge, this is the first report for growing doped $TiO_2$ single crystals employing ion-exchangeable titanate nanotubes as a precursor material. This approach may have a strategic importance for the study and understanding of the electronic properties of different polymorphs of doped $TiO_2$.

Details of the synthesis and characterisation of the materials used in this study can be found in the supplementary material.[16]

Figures 1(a) and 1(c) show the photography and the SEM image of the obtained $TiO_2$ single crystals. The transmission electron microscopy image of cobalt doped titanate nanotubes can be seen in the micrographs of Figure 1(b). A characteristic tubular structure with ca. 10 nm outer- and 5 nm inner-diameter can be observed. The interlayer spacing is 5 Å which is close to the value reported in the literature.[17] X-ray diffraction (XRD) measurement confirms the phase purity of the nanotubes (Fig. 2(a)). No indication of a secondary phase, e.g., metallic cobalt or different cobalt oxides, has been seen within the limit of detection of the technique. It is expected that the $Co^{2+}$ ions were adsorbed onto the surface as well as intercalated into the gallery spacing of the mesoporous material. During CVT, the single crystal nucleation started on the wall of the quartz ampoule. Hundreds of crystals were grown during 14 days, of which a dozen reached even the millimetre size. XRD measurement demonstrates that our single crystals appear in the rutile phase (Fig. 2(a)). It is interesting to note that although the temperature of the growth thermodynamically must have been in favour of the anatase phase, surprisingly here, only the rutile phase was obtained.[18] The growth was repeated several times to confirm the observation. The preference for the growth of the rutile phase might come from the fact that the $NH_4Cl$ transport agent transfers the Co much faster than the Ti-oxide. The Co-oxide creates a template on the cold end of the ampule, which favours the rutile structure. This difference in the transfer rate can explain the much lower concentration of Co in the crystal than in the starting titanate nanotubes (see below).

The concentration of the Co atoms in the precursor materials and in the crystals was determined by energy dispersive X-ray (EDX) and ESR. The concentration in the Co:NTs and Co:TNTs is 2.8% as it is given by EDX. In the crystals, this method is not sensitive enough to detect the
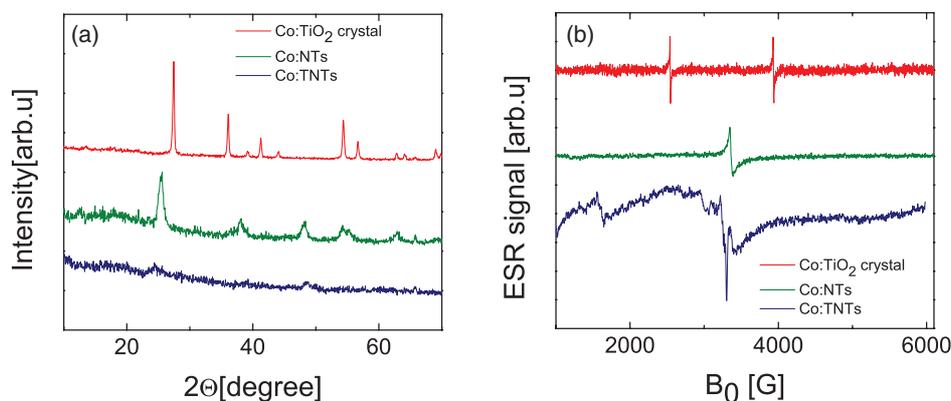
FIG. 2. (a) Powder XRD diffraction of Co doped titanate nanotubes (blue), Co doped titania (green), and the Co doped rutile $TiO_2$ single crystals (red) grown from the titania nanotubes. (b) ESR signal of Co doped titanate nanotubes (blue), Co doped titania (green), and the Co doped rutile $TiO_2$ single crystals (red) grown from the titania nanotubes. ESR spectra are normalized to match the amplitude and shifted vertically for clarity.

low concentration of the dopants, implying that the Co concentration present in the crystals was lower than 0.4%. Thus ESR was used which has much higher sensitivity for magnetic Co dopants (Fig. 2(b)).

The magnetic characterisations were made by field cooled (FC) and zero field cooled (ZFC) SQUID measurements at B = 2 T. For the single crystals, the signal to noise ratio was low due to the low Co concentration and meaningful data could only be recorded in the 4–170 K temperature range (Fig. 3(c)). Similarly, magnetization measurements on 92 mg powdered Co:TNTs and on 33 mg Co:NTs were performed in the entire 3–300 K temperature range (Figs. 3(a) and 3(b), respectively). The room temperature magnetization of Co:TNT is in good agreement with the expectations of 2.8% concentration of octahedral $3d^5$ S = 5/2 $Co^{2+}$ spins. However, the magnetization at room temperature is about 75% higher for Co:TNTs than in the case of the Co:NTs despite the fact that SEM-EDX found the same Co/Ti ratio. Thus, the reduction of magnetization is a consequence of change in the Co spin state from S = 5/2 to S = 1 during the Co:TNT to Co:NT transformation. During the heat treatment to form Co:NTs, the Co ions oxidize to $3d^4$ state $Co^{3+}$. Moreover, due to the increase of the Co ion charge, the magnitude of the crystal field splitting also increases, thus a low-spin S = 1 state forms. This reduction of the magnetic moment is seen by SQUID. The magnetization of the single crystal drops further by a factor of 17 relative to Co:NTs. This is due to the drop of Co concentration in good agreement with the EDX measurements. The temperature dependence of M at high temperatures is paramagnetic-like for both the Co:TNTs and Co:NTs and for the $Co:TiO_2$ crystals. However, the magnetization deviates from the paramagnetic behaviour below T = 140 K for the Co:TNTs and Co:NTs powders, and below T = 30 K for the Co doped $TiO_2$ crystals. This is best seen in the M*T versus T plots in the insets of Figs. 3(a)–3(c). The down turn in the magnetization is characteristic to short range antiferromagnetic fluctuations, however no magnetic ordering was found down to 3 K; the lowest temperatures in our experiments.

The magnetic characterisations were completed by room temperature ESR spectroscopy at 9.4 GHz. At room temperature, the ESR spectra of 38.4 mg Co:TNTs powder revealed a broad $\Delta H$ = 61 mT line with g = 2.22, and a smaller intensity line with a resonance field approximately half of the main line (Figure 2(b), blue). This is characteristic to high Co concentrations in the titanate nanotubes where strong dipole-dipole interaction between the neighbouring $Co^{2+}$ ions broadens the ESR and produces the forbidden transition at half field relative to the paramagnetic position. Additionally, ESR revealed only a very weak, spin = 1/2 impurity signal at g = 2 with $\Delta H$ = 2 mT attributed to 1 ppm paramagnetic defects. Conversely, for 7 mg Co:NTs powder, a single $\Delta H$ = 5 mT line with g = 2 (Figure 2(b), green) was found. The anisotropic shape of the line indicates a weak axial g-factor distribution characteristic to paramagnetic defects. The Co signal was not found in agreement with SQUID, since the $Co^{3+}$ ions are ESR-silent.[19] ESR of 1.15 mg Co doped $TiO_2$
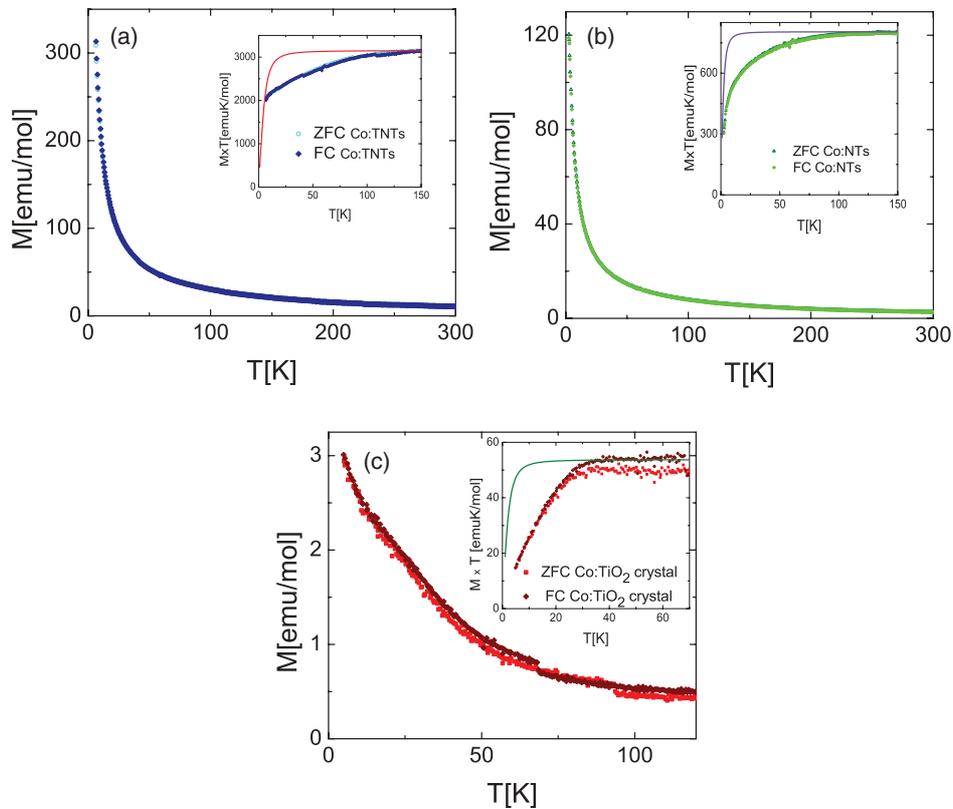
FIG. 3. Magnetization as a function of temperature of Co doped titanate nanotubes (a), Co doped titania (b), and the Co doped rutile TiO$_2$ single crystals (c). The insets give the M*T versus temperature dependences for the three compounds. Line corresponds to a Brillouin function of S = 5/2 paramagnetic spins at B = 2 T in case of Co:TNTs. For Co:NTs and single crystals, a Brillouin function of S = 1 paramagnetic spins at B = 2 T is shown.

crystal is plotted in Figure 2(b) in red. Two low-intensity narrow ΔH = 1 mT ESR resonances were detected. The low signal intensity reveals about 50 ppm spin concentration. The lines are split by 139 mT. This is characteristic for spin-1 species with g = 2.075 and D = 2 GHz axial single ion anisotropy. The absence of the Co ESR in the crystalline form indicates that the oxidation state of Co remained in the 3+ oxidation state (see Ref. 19).

The temperature dependence of the resistivity was measured in the 10–300 K range (Figure 4). One can distinguish two different temperature regimes: (i) an insulating phase between 10 and 50 K, and (ii) a metallic phase for temperatures above 50 K.

The low temperature resistivity can be analysed by the activated behaviour of the resistivity:

$$\rho(T) = \rho_0 e^{\frac{\Delta}{k_B T}}, \tag{1}$$

where $\rho_0$ contains the total carrier concentration participating in the charge transport and the carrier mobility, $k_B$ is the Boltzman's constant, and $\Delta$ is the activation energy for the charge transport. The slope of the log($\rho$) *vs.* 1/T at (see inset to Fig. 4) yields $\Delta$ of 12 meV (140 K). Since it is well known that rutile has an intrinsic band gap of 3 eV,[20] such a low $\Delta$ must reflect the existence of an impurity level within the band gap. The negative Seebeck coefficient (see Figure 5) indicates that it is a low lying donor level situated 12 meV below the conduction band minimum.

For temperatures above 50 K, a few observations should be emphasized: (i) the metal-like temperature dependence of the resistivity characterized by d$\rho$/dT > 0; (ii) the high absolute value of $\rho \approx 5$ $\Omega$ cm – much above the Ioffe Regel limit for metallic conduction; (iii) and the saturation of the resistivity (d$\rho$/dT → 0) for temperatures above 200 K. These characteristics point to a non-standard charge transport mechanism.
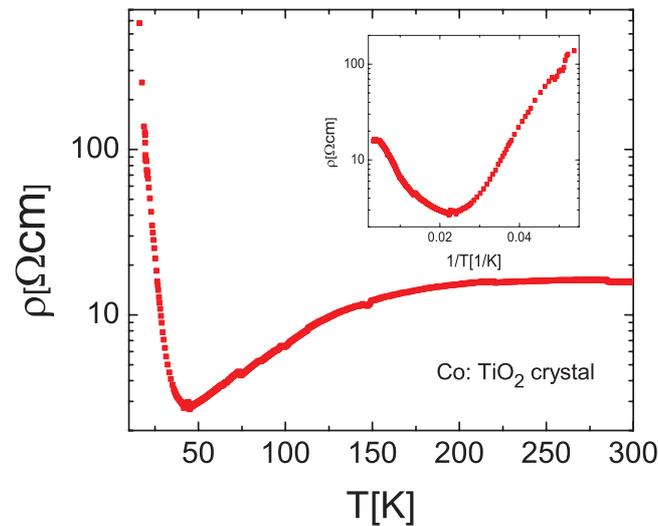
FIG. 4. Resistivity as a function of temperature for Co doped rutile TiO$_2$. The inset shows the Arrhenius plot of the resistivity.
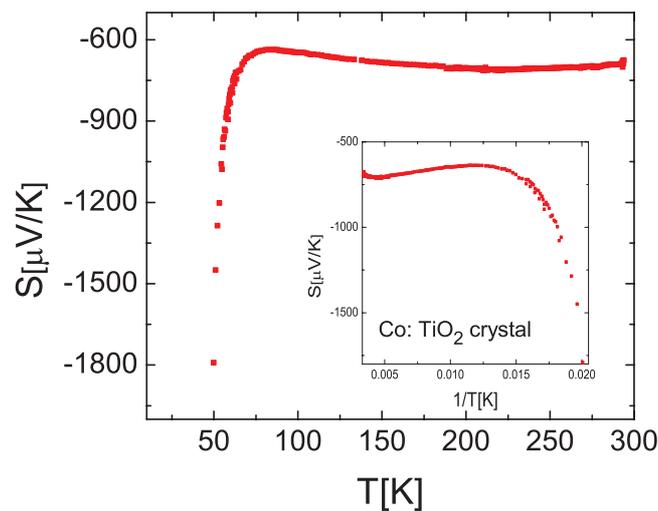


FIG. 5. Thermo-electric power of cobalt doped rutile TiO$_2$ measured as a function of temperature. The inset shows S vs 1/T plot to emphasize the low temperature part.

The donor level might have two origins. In the case of Co doping, replacing Ti$^{4+}$ with Co$^{3+}$ corresponds to adding an electron to the lattice. Oxygen vacancies also donate electrons, which could be thermally activated into the conduction band (CB). One cannot deconvolute the contribution of each of them. Above 50 K their number is high enough in the CB and they give the metallic-like temperature dependence of the resistivity. We have to emphasize that up to our knowledge this is the first doped rutile for which the resistivity has a positive slope. Various doping schemes in the past could reduce the resistivity of rutile considerably, but never showed a metallic resistivity. Its saturation at higher temperature is also a new phenomenon, not yet observed in doped TiO$_2$ (including the anatase phase). Could it come from elastic scattering centres? The dopant sites represent charged scattering centres and they can act as traps for electrons.[21] Since their concentration is low (of the order of $5.4 \times 10^{19}$ cm$^{-3}$),[22] they could not be alone at the origin of the high absolute value of the resistivity and of its tendency for saturation. We suggest that this unusual temperature dependence is coming from the scattering of polaronic quasiparticles by optical phonons. In the anatase phase of TiO$_2$, the existence of polarons has been demonstrated

recently.[23,24] It is reasonable to suppose that in the rutile phase the polaronic interactions are strongly present.[25,26] However, the contribution to the resistivity of the scattering of large polarons on optical phonons has not yet been elaborated upon in theory. This will be the subject of future studies.

The polaronic nature of the charge carriers is best illustrated by thermo-electric power measurements, which give the Seebeck coefficient (S). We measured its temperature dependence in the 30–300 K range. The results are presented in Figure 5. The rather high value of S, around 700 $\mu$V/K, and the weak temperature dependence for T > 100 K corroborate with the non-standard resistivity behaviour. For a metal, S would depend linearly on temperature, whereby it would go as 1/T for a semiconductor. In our interpretation, the high value and the weak temperature dependence are the signature of polaronic charge carriers, as it was elaborated in details by Emin.[27] In a nut-shell, the high value is coming from the lattice softening due to the strong electron-phonon interaction, which increases the vibrational entropy and contributes in the increase of S. Additionally, Seebeck coefficient depends on the mechanism of the charge transport, i.e., on the way the deformation energy is carried in temperature. Below 50 K the freezing out of the electrons necessary for the large polaron formation switches the temperature dependence of S to conventional semiconducting behaviour (see inset to Figure 5).

We have successfully grown millimeter-sized crystals of Co doped rutile by chemical vapour transport using scroll-type Co doped $TiO_2$ nanotubes as a precursor obtained by decomposition of $Co_xH_{2-x}Ti_3O_7$ nanotubes. It opens the possibilities to study the fundamental questions of polaron formation and transport in polar media. From the point of view of applications, the large Seebeck coefficient is promising for a design of thermoelectric devices. For having a large power factor, one has to work on lowering the electrical resistivity of the Co doped rutile.

[1] E. Horvath, P. R. Ribic, F. Hashemi, L. Forro, and A. Magrez, J. Mater. Chem. **22**(18), 8778–8784 (2012).

[2] J. Jacimovic, R. Gaal, A. Magrez, J. Piatek, L. Forro, S. Nakao, Y. Hirose, and T. Hasegawa, Appl. Phys. Lett. **102**(1), 013901–13901 (2013).

[3] N. Tetreault, E. Horvath, T. Moehl, J. Brillet, R. Smajda, S. Bungener, N. Cai, P. Wang, S. M. Zakeeruddin, L. Forro, A. Magrez, and M. Gratzel, ACS Nano **4**(12), 7644–7650 (2010).

[4] M. Hodos, E. Horvath, H. Haspel, A. Kukovecz, Z. Konya, and I. Kiricsi, Chem. Phys. Lett. **399**(4–6), 512–515 (2004).

[5] L. R. Sheppard, T. Bak, and J. Nowotny, J. Phys. Chem. C **112**(2), 611–617 (2008).

[6] Y. Matsumoto, M. Murakami, T. Shono, T. Hasegawa, T. Fukumura, M. Kawasaki, P. Ahmet, T. Chikyow, S. Koshihara, and H. Koinuma, Science **291**(5505), 854–856 (2001).

[7] J. M. D. Coey, Curr. Opin. Solid State Mater. Sci. **10**(2), 83–92 (2006).

[8] R. Janisch, P. Gopal, and N. A. Spaldin, J. Phys. Condens. Matter **17**(27), R657–R689 (2005).

[9] T. Fukumura, Y. Yamada, H. Toyosaki, T. Hasegawa, H. Koinuma, and M. Kawasaki, Appl. Surf. Sci. **223**(1–3), 62–67 (2004).

[10] M. Murakami, Y. Matsumoto, T. Hasegawa, P. Ahmet, K. Nakajima, T. Chikyow, H. Ofuchi, I. Nakai, and H. Koinuma, J. Appl. Phys. **95**(10), 5330–5333 (2004).

[11] J. Y. Kim, J. H. Park, B. G. Park, H. J. Noh, S. J. Oh, J. S. Yang, D. H. Kim, S. D. Bu, T. W. Noh, H. J. Lin, H. H. Hsieh, and C. T. Chen, Phys. Rev. Lett. **90**(1), 017401 (2003).

[12] P. Triggs, H. Berger, C. A. Georg, and F. Levy, Mater. Res. Bull. **18**(6), 677–681 (1983).

[13] A. Kukovecz, N. Hodos, E. Horvath, G. Radnoczi, Z. Konya, and I. Kiricsi, J. Phys. Chem. B **109**(38), 17781–17783 (2005).

[14] P. Szirmai, E. Horvath, B. Nafradi, Z. Mickovic, R. Smajda, D. M. Djokic, K. Schenk, L. Forro, and A. Magrez, J. Phys. Chem. C **117**(1), 697–702 (2013).

[15] E. Horvath, A. Kukovecz, Z. Konya, and I. Kiricsi, Chem. Mater. **19**(4), 927–931 (2007).

[16] See supplementary material at http://dx.doi.org/10.1063/1.4820438 for a description of the materials synthesis and characterisation.

[17] Q. Chen, G. H. Du, S. Zhang, and L. M. Peng, Acta Crystallogr., Sect. B: Struct. Crystallogr. Cryst. Chem. **58**, 587–593 (2002).

[18] H. Berger, H. Tang, and F. Levy, J. Cryst. Growth **130**(1–2), 108–112 (1993).

[19] C. Montes, M. E. Davis, B. Murray, and M. Narayana, J. Phys. Chem **94**(16), 6425–6430 (1990).

[20] D. C. Cronemeyer, Phys. Rev. **87**(5), 876–886 (1952).

[21] R. R. Heikes and W. D. Johnston, J. Chem. Phys. **26**(3), 582–587 (1957).

[22] Assuming that only Co cations were doping the system, the carrier concentration can be estimated as $5.4 \times 10^{19}$ $cm^{-3}$ from the ESR intensity.

[23] J. Jacimovic, C. Vaju, A. Magrez, H. Berger, L. Forro, R. Gaal, V. Cerovski, and R. Zikic, EPL **99**(5), 57005 (2012).

[24] S. Moser, L. Moreschini, J. Jacimovic, O. S. Barisic, H. Berger, A. Magrez, Y. J. Chang, K. S. Kim, A. Bostwick, E. Rotenberg, L. Forro, and M. Grioni, Phys. Rev. Lett. **110**(19), 196403 (2013).
[25] D. M. Eagles, J. Phys. Chem. Solids **25**(11), 1243 (1964).
[26] C. Persson and A. F. da Silva, Appl. Phys. Lett. **86**(23), 231912 (2005).
[27] D. Emin, Phys. Rev. B **59**(9), 6205–6210 (1999).